

NCC 2-5259

50th Meeting of the AEROBALLISTIC RANGE ASSOCIATION  
Pleasanton, California, November 8 - 12, 1999.

**Current Testing Capabilities at the  
NASA Ames Ballistic Ranges**

by

Alvin Ramsey  
University of California, Berkeley  
Berkeley, CA 94720

Tim Tam  
NASA Ames Research Center  
Moffett Field, CA 94035

David Bogdanoff  
Eloret  
Moffett Field, CA 94035

Peter Gage  
Eloret  
Moffett Field, CA 94035

NOV 15 1999

CL: 202A-3

CASI

GRANT  
IN-09

**ABSTRACT**

Capabilities for designing and performing ballistic range tests at the NASA Ames Research Center are presented. Computational tools to assist in designing and developing ballistic range models and to predict the flight characteristics of these models are described. A CFD code modeling two-stage gun performance is available, allowing muzzle velocity, maximum projectile base pressure, and gun erosion to be predicted. Aerodynamic characteristics such as drag and stability can be obtained at speeds ranging from 0.2 km/s to 8 km/s. The composition and density of the test gas can be controlled, which allows for an assessment of Reynolds number and specific heat ratio effects under conditions that closely match those encountered during planetary entry. Pressure transducers have been installed in the gun breech to record the time history of the pressure during launch, and pressure transducers have also been installed in the walls of the range to measure sonic boom effects. To illustrate the testing capabilities of the Ames ballistic ranges, an overview of some of the recent tests is given.

**INTRODUCTION**

Currently there are two functioning ballistic ranges at the NASA Ames Research Center. The aerodynamic range, which first became operational in 1965, is used to measure steady and unsteady aerodynamic coefficients of projectiles. The gun development range, originally constructed in 1964, is used for gun performance enhancements and gas radiation studies.

The ballistic ranges at the NASA Ames Research Center has been recently renovated to provide improved testing capabilities for research, and a number of test programs have exploited these new capabilities. This paper presents the current ballistic range testing capabilities at the NASA Ames Research Center. In addition to the capabilities of the ballistic ranges, design tools are available that allow the entire design, testing, and data

reduction process to be performed at Ames in several months. First, the experimental design capabilities are presented, followed by a description of the ballistic ranges. Finally, an overview of some of the recent test programs will serve to illustrate the testing capabilities and the type of data obtained.

### **EXPERIMENTAL DESIGN CAPABILITIES**

Various tools and resources are available at the NASA Ames Research Center to assist in the design and development of ballistic range tests. Computer Aided Design (CAD) tools are used to design complex ballistic range models; these are integrated with in-house precision machining capabilities. CFD capabilities are used to predict aerodynamic characteristics and real gas flow physics. Also, a CFD model has been developed for two-stage light gas gun cycles which incorporates gun erosion effects. These tools are employed to design ballistic range models and to predict test results of firings in the range.

*CAD Tools:* CAD tools have been used to develop ballistic range models of various degrees of complexity at Ames. The CAD software used is ProEngineer<sup>®</sup>,<sup>1</sup> which is a powerful software package used by both designers and machinists at Ames. Some of the more complex models fired in the range necessitated using CAD for the model designs and the calculations of the mass properties such as the center of gravity location and moments of inertia. One such model is shown in Figure 1. The model has a conical tip with struts attached to a cowl that forms a channel, allowing the oncoming air to flow through the nose and to exit at the cowl end. The model consists of the body, cowl, and the struts to support the cowl; all fabricated in the precision machine shop at Ames. The CAD tools are integrated into the precision machine shop at Ames to design and fabricate intricate models.

*CFD Capabilities:* The primary software package used to perform CFD analysis is the General Aerodynamic Simulation Program (GASP).<sup>2</sup> GASP is an established commercial Navier-Stokes flow solver that has a number of built-in turbulence and chemistry models. Integrated quantities such as lift and drag are computed from the resultant flow field solution. These aerodynamic quantities are used to predict the flight behavior of low and high speed ballistic range shots. An example of CFD results is given in Figure 2, which displays the Mach number profile computed for the channeled model.

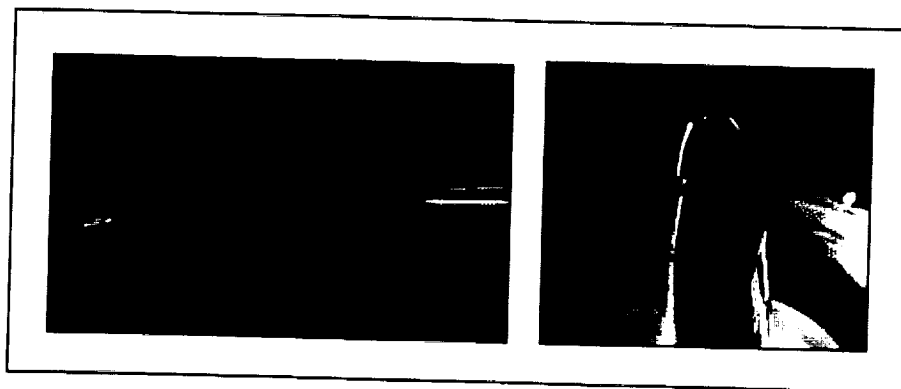


**Figure 1. Images of the channeled model.**

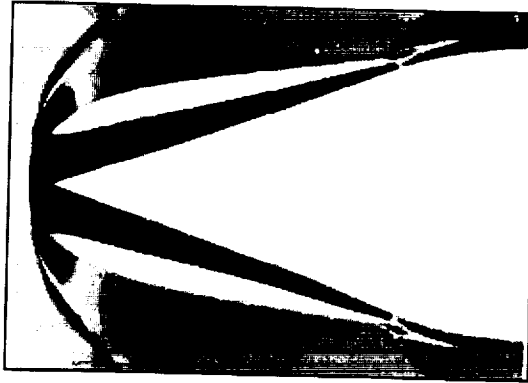


**Figure 2. CFD results of a channeled model.**

*CFD Model for Two-stage Light Gas Gun Cycles:* A CFD code<sup>3</sup> for the analysis of the internal ballistics of two-stage light gas guns is available. The code has been extensively validated against projectile and piston velocity data, powder chamber and pump tube pressure data and erosion data from the facility's 0.5 inch and 1.5 inch guns. The code enables the user to select gun operating conditions to produce the desired muzzle velocity while minimizing the maximum pressure and shock wave amplitudes at the projectile base. In addition, the maximum pressures in the high pressure contraction section of the gun and gun erosion are calculated. For high performance shots, the gun operating conditions are chosen to insure reasonable life of the gun and for the high pressure contraction section and gun barrel.

## **TESTING CAPABILITIES**

There are two ballistic ranges currently operational at Ames: the aerodynamic range and the gun development range. The aerodynamic range is used primarily to obtain the aerodynamic characteristics such as drag and stability of the projectiles. The gun development range is employed for assessing enhancements of gun performance and for gas radiation studies. A wide variety of experiments can be performed in the ballistic ranges at Ames. Table 1 presents the specifications of both ranges and Table 2 presents the launchers available in the ranges. Table 3 gives the measurement errors associated with the aerodynamic range.

## **DESCRIPTION OF RECENT TESTS**

The following section serves to illustrate the uses of some of the capabilities of the ranges by describing the recent tests that were performed:

*Calibration Spheres:* Calibration shots are performed periodically in the range by shooting steel spheres under vacuum conditions. In the absence of air, gravity is the only force acting upon the sphere and thus the trajectory of the sphere can be calculated precisely. The expected trajectory is compared with the measured trajectory to calculate the bias errors of the range position measurements, which will be used for correcting later aerodynamic data. Calibration shots have been launched at speeds up to 6 km/s. Figure 3 shows an X-ray photograph of the onset of sabot separation during a calibration sphere shot in the gun development range.<sup>4</sup>

**Table 1. Description of ranges currently operational at Ames.**

	AMES BALLISTIC RANGE	
	<i>Aerodynamic Range</i>	<i>Gun Development Range</i>
<b>Primary use</b>	To measure aerodynamic coefficients of projectiles	Gun performance enhancement and gas radiation studies
<b>Length</b>	30 m.	11 m.
<b>Range test medium</b>	Air, CO <sub>2</sub> , N <sub>2</sub> , Ar, Kr, or other gases	Air, CO <sub>2</sub> , N <sub>2</sub> , Ar, Kr, or other gases
<b>Diagnostics and special capabilities</b>	<ul style="list-style-type: none"> <li>• 16 stations with orthogonal shadowgraph capability (30-38 cm aperture); Kerr cells used to block self-luminosity of projectile</li> <li>• 13 wall-mounted pressure transducers for sonic boom studies at nine different stations</li> </ul>	<ul style="list-style-type: none"> <li>• Four photomultiplier-based velocity stations</li> <li>• Three flash X-ray stations for monitoring sabot separation, impact, etc.</li> <li>• Spectroscopic equipment for radiation studies</li> </ul>

**Table 2. Description of launchers available in the ranges.**

<b>Two-stage Light Gas Guns</b>	<b>Powder Guns</b>
<ul style="list-style-type: none"> <li>• Barrel diameters - 7.1 mm, 12.7 mm, 25.4 mm, 38 mm.</li> <li>• Muzzle velocities <ul style="list-style-type: none"> <li>– slugs up to 9-9.5 km/sec.</li> <li>– sabot models up to 8-8.5 km/sec.</li> </ul> </li> </ul>	<ul style="list-style-type: none"> <li>• Five guns available, barrel diameters up to 61 mm.</li> <li>• Muzzle velocities up to 2.7 km/sec.</li> </ul>

**Table 3. Estimated errors associated with the aerodynamic range.**

Estimated down range error ( $x$ )	0.01 in.
Estimated swerve error ( $y, z$ )	0.01 in.
Estimated angular error ( $\theta, \psi$ )	0.01°
Estimated roll error ( $\phi$ )	1.0°

*Sphere-cones - Solid and Channeled:* A concept for reducing sonic boom with minimal drag penalty has been tested at Ames. The concept incorporates a channel for flow to enter at the nose of the vehicle. Figure 4 illustrates the concept applied to a sphere-cone geometry.

A method was required to measure the sonic boom as the model flew down the range. Pressure transducers were mounted in the walls at several locations in the ballistic range to measure the pressure trace of the sonic boom. Figure 5 shows two graphs that illustrate the difference in the sonic boom strength between the solid sphere-cone and the channeled sphere-cone models. The shape of the pressure signal is due to the leading and

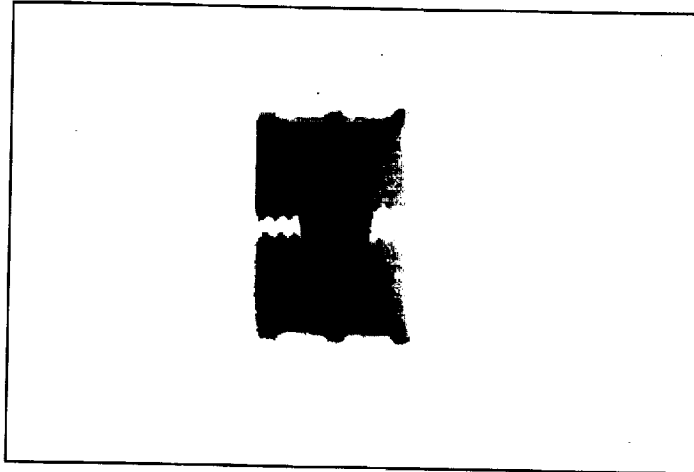


Figure 3. X-ray photograph of sabot separation for a calibration sphere shot.

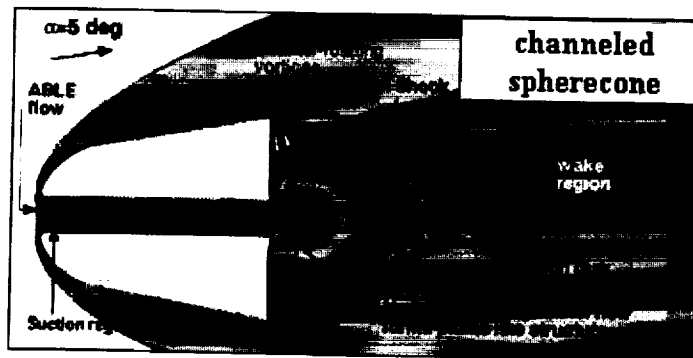


Figure 4. Cross-sectional view of a channeled sphere-cone model.

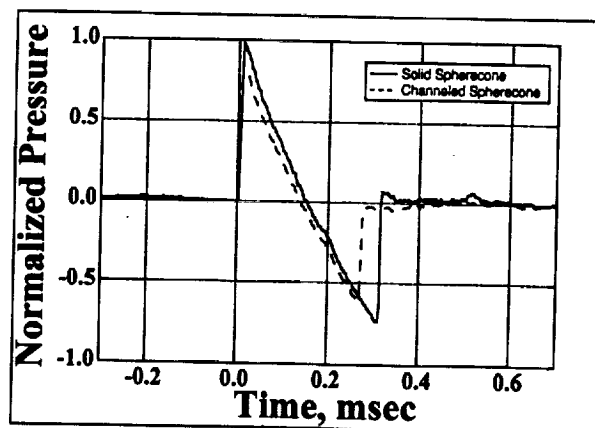


Figure 5. Pressure traces of the sonic boom for the solid and channeled sphere-cone.

trailing shock wave of the model. The solid line represents the pressure trace of a solid sphere-cone shot past one of the stations and the dashed line represents the pressure trace at the same station for a channeled sphere-cone model. The channeled sphere-cone produced a peak-to-peak pressure difference that was 16% less than the peak-to-peak

pressure difference of the solid sphere-cone, which demonstrated the effectiveness of the channel. Pressure was normalized to comply with nondisclosure agreements with the contractor.

**ABLE Models:** The concept of reducing sonic boom and minimizing drag from the channeled sphere-cones has been developed further with the Artificially Blunted Leading Edge (ABLE) models.<sup>5</sup> To increase the usable payload volume, the channel has been essentially redirected from the centerline of the sphere-cone to the sides. Implementation of this concept resulted in a design having a cowl attached to a sharp cone via struts, with the cowl and strut assembly forming a channel from the projectile's nose to an annular outlet at the rear of the cowl. Several different cowl lengths were used in testing the ABLE concept. Figure 1 illustrates the short cowl model and Figure 6 shows the long cowed model.

**SHARP:** Hankey and Elliot<sup>6</sup> determined optimal lifting hypersonic configurations that produced maximum lift-drag ratios using volumetric efficiency and a nose-heating limit as constraints. Implementation of the concepts resulting from this work led to the geometry shown in Figure 7. A series of models and sabots for this non-axisymmetric geometry have been designed, manufactured, and tested in the ballistic range at Ames.

**Stardust Space Probe:** A current research effort in progress at Ames is the assessment of how the afterbody geometry affects the stability of entry probes. One phenomenon occurring with entry probes in free-flight is the presence of a limit cycle, which is the occurrence of persistent oscillations with amplitudes approaching a limit. For a blunted cone, Sammonds<sup>7</sup> found that a spherical afterbody with the center of curvature located at the probe's center of gravity would reduce the amplitude of the limit cycle normally experienced during flight. Chapman, et al.<sup>8</sup> further explored the concept with ballistic range tests of the Huygens probe.

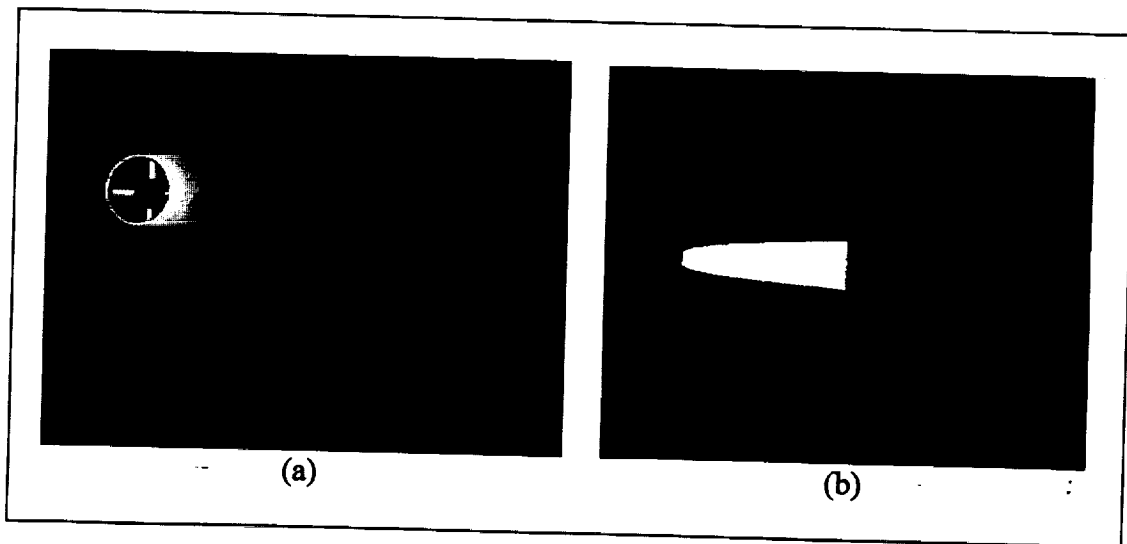


**Figure 6. Long cowed ABLE model (a) CAD assembly drawing and (b) shadowgraph.**

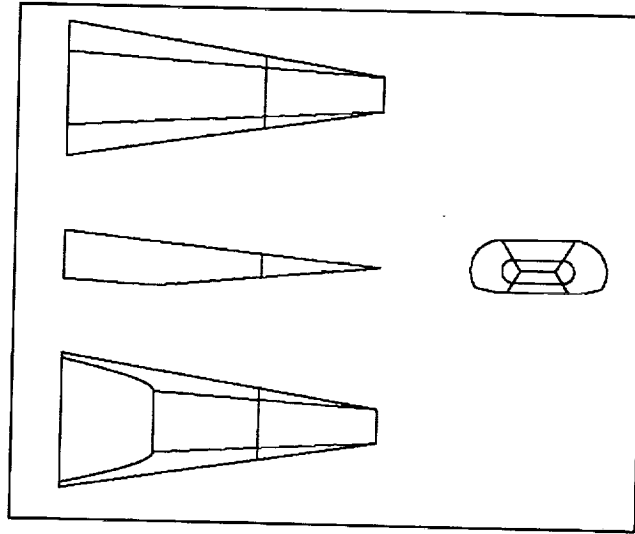


**Figure 7. Schematic of the SHARP configuration.**

At Ames, the Stardust probe geometry was selected for the study, and some of the following points of interests were addressed:

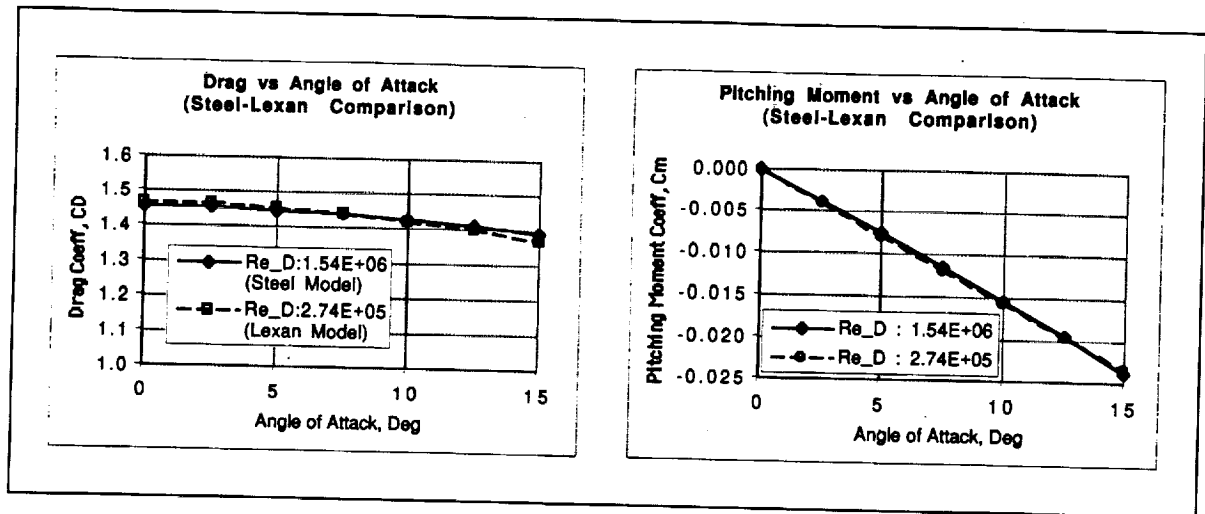
- What are the static and dynamic aerodynamic characteristics of the Stardust geometry?
- What are the Reynolds number ( $Re_D$ ) effects on the static and dynamic aerodynamics?
- How is the dynamic stability affected the Stardust afterbody is made spherical?
- Are there other afterbody shapes that also reduce the amplitude of the limit cycle?

Table 4 shows the test program implemented for the Stardust configuration. Six of the 13 ballistic range models that were tested were made from steel, while the other seven were made from Lexan plastic. The pressure of the test gas in the range was altered to maintain the density ratio between the model and the test gas, which resulted in the  $Re_D$  being different in the test conditions between the steel and the Lexan models. Results given in Figure 8 show that the steel and the Lexan models behaved similarly, despite nearly an order of magnitude difference in  $Re_D$  between the two sets of shots.

Two of the Lexan models were shot at higher pressures which increased the number of cycles of motion in the range from 2 to 3 by increasing the aerodynamic moments experienced by the models. The increased number of cycles for the two Lexan models

**Table 4. Test program of the Stardust geometry.**

Material	No. of Shots	No. of Cycles in Range	Pressure of Test Gas	$Re_D$
Steel	6	2	1.000 atm.	$1.54 \times 10^6$
Lexan	5	2	0.178 atm.	$2.74 \times 10^5$
Lexan	2	3	0.401 atm.	$6.18 \times 10^5$



**Figure 8. Comparisons of the aerodynamic coefficients at two different Reynolds numbers for the Stardust models.**

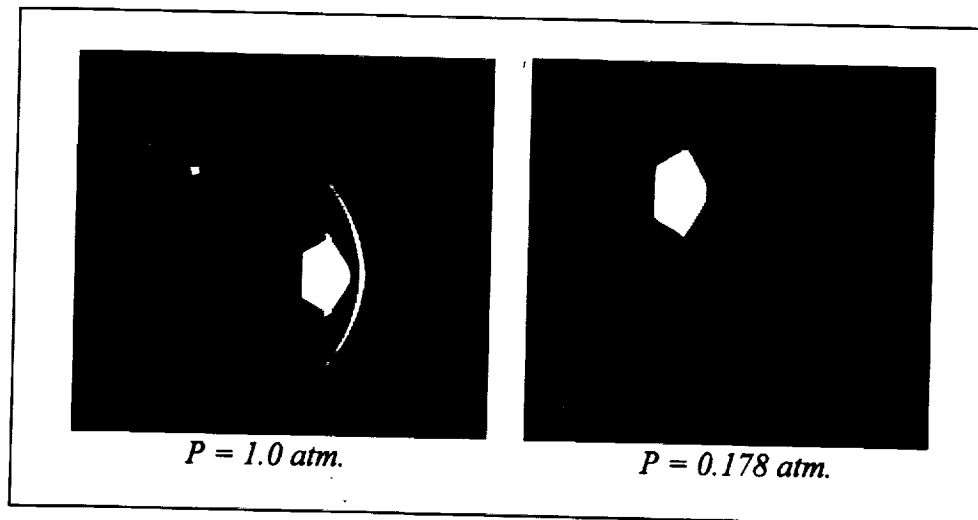


**Figure 9. Comparison of shots in 1.0 atm. and 0.178 atm.**

increased the accuracy of assessing the dynamic stability by providing more information to the data reduction routine. The test gas for this series of shots was air; future tests may use  $\text{CO}_2$  as the test gas to study the effects of different specific heat ratios on the aerodynamics. Figure 9 compares the shadowgraphs obtained from shots in atmospheric and sub-atmospheric pressures. The flow details are readily visible in the shot at 1.0 atm. pressure, while only the bow shock can be seen from the shot at the lower pressure.

## CONCLUSION

The ballistic ranges at Ames have many testing capabilities for low and high speed shots. The aerodynamic range can be used to perform tests with a variety of test gases at pressures from atmospheric to near vacuum levels. The gun development range can be used to study enhancements of gun performance and gas radiation from shock layers. The Ames aerodynamic and gun development ranges provide unique capabilities for



ballistic range testing for NASA and industry collaborative programs. A number of these capabilities have been reviewed herein and results from several recent tests have been discussed.

## REFERENCES

- <sup>1</sup> Anon., *ProEngineer® Fundamentals Release 18.0*, Parametric Technology Corporation, Waltham, MA, 1997.
- <sup>2</sup> Walters, R. W., et al., "GASP Version 3, The General Aerodynamic Simulation Program User's Manual," AeroSoft, Inc., May 1996.
- <sup>3</sup> Bogdanoff, D. W., "CFD Modelling of Bore Erosion in Two-Stage Light Gas Guns," presented at the 49th Aeroballistic Range Association Meeting, Scheveningen, the Netherlands, October 5 - 9, 1998.
- <sup>4</sup> Bogdanoff, D. W., Miller, R. J., "Recent Developments in Gun Operating Techniques at the NASA Ames Ballistic Ranges," NASA TM-110387, Mar. 1996.
- <sup>5</sup> Gupta, A., Ruffin, S. M., Newfield, M. E., and Yates, L. A., "Aerothermodynamic Performance of Sphere-Cones Using the Artificially Blunted Leading Edge Concept," *AIAA Aerospace Sciences Meeting and Exhibit*, Reno, NV, Jan. 11-14, 1999, AIAA Paper No. 99-0897.
- <sup>6</sup> Hankey, W. L. and Elliott, G. A., "Hypersonic Lifting Body Optimization," *AIAA Journal of Spacecraft and Rockets*, Vol. 5, No. 12, Dec 1968, pp. 1463-1467.
- <sup>7</sup> Sammonds, R. I., "Transonic Static and Dynamic Stability Characteristics of Two Large-Angle Spherically-Blunted High-Drag Cones," *AIAA Atmospheric Flight Mechanics Conference*, Tullahoma, TN, May 13-15, 1970, AIAA Paper No. 70-564.
- <sup>8</sup> Chapman, G.T, Berner, C., Winchenbach, G. L., Hathaway, W. H., and Mitcheltree, R. A., "The Use of Spherical Bases to Eliminate Limit Cycles of Blunt Entry Vehicles," *37th AIAA Aerospace Sciences Meeting and Exhibit*, Reno, NV, Jan. 11-14, 1999, AIAA Paper No. 99-1023.